IEEE Photonics Journal
An IEEE Photonics Society Publication

Open Access

Neutral Mounting of Ultrahigh Q Whispering Gallery Mode disc-Resonators for Metrological Applications

Volume 9, Number 1, February 2017

Yanne K. Chembo, ***Senior Member, IEEE***
Lukas Baumgartel
Nan Yu

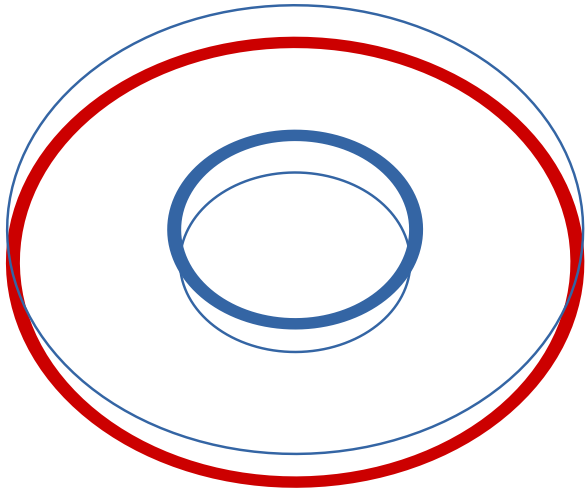

DOI: 10.1109/JPHOT.2016.2638041
1943-0655 © 2016 IEEE

IEEE photonics SOCIETY

IEEE

Neutral Mounting of Ultrahigh Q Whispering Gallery Mode disc-Resonators for Metrological Applications

Yanne K. Chembo,[1] ***Senior Member, IEEE*, Lukas Baumgartel,**[2] **and Nan Yu**[2]

[1]FEMTO-ST Institute, Optics Department, CNRS and Université Bourgogne-Franche-Comté, 25030 Besançon cedex, France
[2]Jet Propulsion Laboratory, California Institute of Technology, Pasadena, CA 91109 USA

DOI:10.1109/JPHOT.2016.2638041
1943-0655 © 2015 IEEE. Translations and content mining are permitted for academic research only. Personal use is also permitted, but republication/redistribution requires IEEE permission. See http://www.ieee.org/publications_standards/publications/rights/index.html for more information.

Manuscript received September 18, 2016; revised November 28, 2016; accepted December 7, 2016. Date of publication December 22, 2016; date of current version January 3, 2017. This work was supported by the Jet Propulsion Laboratory, California Institute of Technology, under a contract with NASA. Corresponding author: Yanne K. Chembo (e-mail: yanne.chembo@femto-st.fr).

Abstract: Whispering gallery mode resonators find key applications in microwave photonic oscillators for aerospace engineering, frequency synthesis, and time-frequency metrology. However, their elastic mechanical deformations induce undesirable shifts for their optical eigenfrequencies, which should ideally be immune to vibrations. We propose a mounting configuration that provides strong immunity against external vibrations and mechanical fluctuations. Numerical simulations confirm the analytical study.

Index Terms: Whispering gallery mode resonator, microwave photonic oscillators, time-frequency metrology.

1. Introduction

Whispering-gallery mode (WGM) disc-resonators are currently at the core of a rapidly thriving research activity. In several applications, WGM resonators are expected to play the role of frequency reference cavities, where a given resonance frequency of the cavity is ideally expected to remain constant, despite the detrimental influence of a fluctuating environment.

The initial trend in investigations related to WGM resonators was to study their linear properties, mainly characterized by its intrinsic Q-factor. In this linear regime, the cavity may perform photon storage or ultra-selective optical filtering, since the quality factor is proportional to the photon lifetime τ, and inversely proportional to the modal linewidth $\Delta\omega_0$, following $Q = \omega_0\tau = \omega_0/\Delta\omega_0$ [1]–[5]. The nonlinear characteristics of WGM resonators have also been the focus of intense research activities, as it has very early been shown that increasing the Q-factor accordingly decreases the value of the threshold pump power required to observe nonlinear phenomena [6]–[8]. Both the linear and nonlinear properties of WGM resonators have paved the way for metrological applications [9]–[14], where the final objective is the generation of exceptionally stable microwave or lightwave radiations. In many of these applications, the frequency stability of the resonator is critical.

From a broader perspective, the resonance frequency ω_0 of a resonator scales as $\omega_0 \propto c/n_g R$, where c is the velocity of light, n_g the group-velocity refraction index at the frequency ω_0, and R is

a characteristic dimension of the resonator. Therefore, fluctuation of n_g and R induce a frequency fluctuation $\delta\omega_0/\omega_0 = -\delta n_g/n_g - \delta R/R$. Hence, fluctuations in the refraction index and the cavity dimensions will be transduced to jitters and drifts in the resonance frequencies. Both internal and environmental fluctuations will ultimately limit the practically achievable frequency stability. It is then required to reduce the fluctuations δR and δn as much as possible.

Such fluctuations may have a thermal origin. They have been theoretically investigated in the scientific literature for WGM disc-resonators [15], [16], and many control strategies have been proposed to stabilize WGM cavities in temperature. In particular, frequency stabilization of lasers locked to passive Fabry-Pérot optical cavities has reached the performance of $\sim 10^{-15}\,\mathrm{Hz}^{-1/2}$ [17], [18], but performances are typically of the order of $\sim 10^{-12}\,\mathrm{Hz}^{-1/2}$ with WGM disc-resonators [19], while the thermal limit has been pushed down to $\sim 10^{-14}\,\mathrm{Hz}^{-1/2}$ [20].

The focus of this article is therefore to analyze this later aspect for the particular case of WGM disc-resonators. Here, the geometrical parameter R defining the resonance frequency is the radius of the disc, and an open problem is to find a way to mount the discs in such a way that this external radius remains stable against vibration and acceleration.

For the case of Fabry-Pérot resonators, research on optimal mounting architectures has been very fruitful. One of the simplest strategies, referred here as *neutral mounting*, has successfully been implemented by Leibrandt *et al.* [21]. Webster and Gill have also proposed force-insensitive optical cavities mounted in cubical structures [22]. In the particular case of neutral mounting, the main conceptual idea is that in some configurations, if two extreme mounting positions induce opposite sign displacements for the geometrical variable ΔR, then there is necessarily an intermediate mounting position for which this displacement is null (intermediate value theorem). For that optimal position, the conversion of external vibrations into cavity deformation is therefore inhibited for the geometrical parameter R of interest, and thereby guarantees high frequency stability.

It is the purpose of this work to propose a similar strategy for WGM disc-resonators, and to evaluate its performance against vibration and acceleration. More precisely, we show that clamping a WGM disc between two coaxial cylinders induces a radial displacement field that is null in a neutral circumference path. This optimal configuration, that is unaffected by the mounting force, can therefore host the WGM resonators and preserve their eigenfrequencies from mechanical fluctuations. This immunity to the external fluctuations is necessary to ensure high stability and coherence of the output signals for the targeted applications [23]–[27].

The organization of this paper is as follows. In Section 2, we briefly present the concept of neutral mounting for optical resonators. Then, we will provide the general description of the analytical approach, which is based on the the Love strain function. Section 3 will focus on specific case studies where zero deformation configuration does exist. Section 4 will be devoted to numerical simulations, and the last section concludes the paper.

2. Analytical Approach of Neutral Mounting

The principle of neutral mounting is explicitly illustrated in Fig. 1. In the optimal configuration of Fig. 1(d), the reference cavity length defining the reference resonance frequency remains unchanged regardless of the intensity of the mounting forces. Hence, both time-varying (vibration) and steady (acceleration) forces have no effect at first order on the frequency of interest. Of course, this conclusion is true if and only if we remain in the elastic regime of the sphere (linear deformations).

Even though easily applicable to spherical WGM resonators [28], the strategy of neutral mounting with disc-resonators is not as obvious as that of Fig. 1, because it should fulfill a certain number of requirements. The most important one is that the rim of the disc (lateral surface) has to be free. Effectively, any mechanical contact with the rim would at the same time degrade the Q-factor and possibly affect the optical circular path of the modes through the circumference deformation. In this latter case, any fluctuation in the mounting force would automatically induce a fluctuation of the optical path, and then, of the resonance frequency.

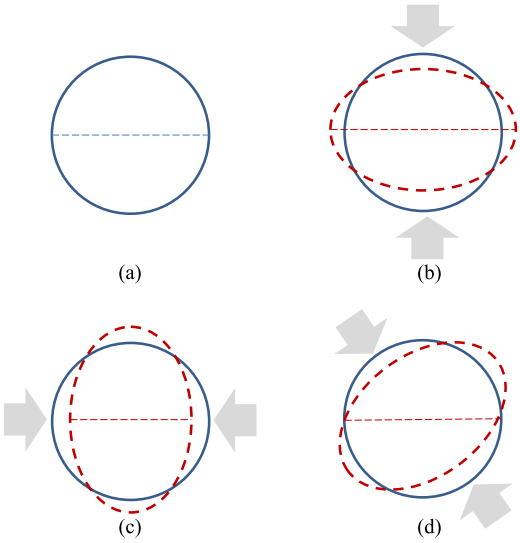

Fig. 1. Principle of neutral mounting, as explained in [21]. The solid (discontinuous) circle (ellipse) stands for the unloaded (loaded) spherical cavity. The arrows indicate the mounting forces. (a) Unloaded sphere, with the horizontal axis (diameter) being the reference length of a Fabry-Pérot cavity. (b) Vertical mounting. The sphere is elongated horizontally, and the reference cavity length is larger. (c) Horizontal mounting. The sphere is elongated vertically, and the reference cavity length is shorter. (d) Neutral mounting. The sphere diameter has a zero displacement along the axis of interest. The mounting force may fluctuate without inducing undesirable cavity length fluctuations.

Theoretical guidance is therefore useful to identify mounting architectures that are likely to fulfill the force-insensitive requirement, while still being compatible with fairly simple experimental implementation.

In general, linear elasticity problems in three dimensions have no analytic solutions. Even the simple problem of an elastic cylinder deformed by its own weight is already very complex (see, for example, [29]). However, uniqueness and existence of solutions to the linear static elasticity equations can be proved under some specific conditions. For example, if only displacements are prescribed on the boundary of the solid, it can proven that a solution exists, and it is unique. The same conclusion can be drawn if mixed boundary conditions (displacements or stresses) are specified. If only stresses (fulfilling equilibrium conditions) are prescribed on the boundary, a static solution exists, that is unique in terms of stresses and strains fields but not in terms of displacements.

It is not the objective of this paper to study with full precision the elastostatic deformations of a disc-resonator. However, the Love function is a useful tool to give an qualitative insight relatively to how a disc is deformed under various mounting schemes [30] and provides a proof of existence of configurations where a null displacement (at first order of approximation) is expected for the radius of the disc.

We can take advantage of the fact that our problem is axial-symmetric. In this case, we use the Love strain function $\mathcal{L}$ which fulfills the biharmonic equation

$$\nabla^2\nabla^2\mathcal{L} = 0 \tag{1}$$

in the case of null body-forces, with $\nabla^2 = \partial_r^2 + r^{-1}\partial_r + r^{-2}\partial_\theta^2 + \partial_z^2$ being the Laplacian operator in cylindrical coordinates. Once the Love strain function $\mathcal{L}$ is known, the displacement, stress, and strain fields can be explicitly determined. In principle, every axisymmetric mounting configuration is characterized by a unique function $\mathcal{L}$ which enables to determine the deformation of the disc [30].

More concretely, the displacement field is obtained as

$$\begin{aligned} u_r &= -\frac{1}{2G}\frac{\partial^2 \mathcal{L}}{\partial r \partial z} \\ u_\theta &= -\frac{1}{2G}\frac{1}{r}\frac{\partial^2 \mathcal{L}}{\partial \theta \partial z} \\ u_z &= \frac{1}{2G}\left[2(1-\nu)\nabla^2 - \frac{\partial^2}{\partial z^2}\right]\mathcal{L} \end{aligned} \tag{2}$$

where $G = E/2(1+\nu)$ is the shear modulus, E is the Young's modulus, and ν is the Poisson's ratio.

On the other hand, the stress tensor field is explicitly recovered through

$$\begin{aligned} \sigma_{rr} &= \frac{\partial}{\partial z}\left[\nu\nabla^2 - \frac{\partial^2}{\partial r^2}\right]\mathcal{L} \\ \sigma_{r\theta} &= -\frac{\partial^3}{\partial r \partial \theta \partial z}\left(\frac{\mathcal{L}}{r}\right) \\ \sigma_{\theta\theta} &= \frac{\partial}{\partial z}\left[\nu\nabla^2 - \frac{1}{r}\frac{\partial}{\partial r} - \frac{1}{r^2}\frac{\partial^2}{\partial \theta^2}\right]\mathcal{L} \\ \sigma_{\theta z} &= \frac{1}{r}\frac{\partial}{\partial \theta}\left[(1-\nu)\nabla^2 - \frac{\partial^2}{\partial z^2}\right]\mathcal{L} \\ \sigma_{zz} &= \frac{\partial}{\partial z}\left[(2-\nu)\nabla^2 - \frac{\partial^2}{\partial z^2}\right]\mathcal{L} \\ \sigma_{rz} &= \frac{\partial}{\partial r}\left[(1-\nu)\nabla^2 - \frac{\partial^2}{\partial z^2}\right]\mathcal{L}. \end{aligned} \tag{3}$$

Finally, knowing the stress tensor $\boldsymbol{\sigma}$, the strain tensor $\boldsymbol{\varepsilon}$ can also be obtained using Hooke's law, following $\boldsymbol{\varepsilon} = [(1+\nu)\boldsymbol{\sigma} - \nu\,\mathrm{Tr}(\boldsymbol{\sigma})\,\mathbf{I}]\,E^{-1}$, where Tr is the matrix trace function, and $\mathbf{I}$ is the identity matrix. It is worth noting that both stress and strain tensors are symmetric, and also that owing to the axial symmetry, we will always restrict ourselves to Love strain function fulfilling $\partial\mathcal{L}/\partial\theta \equiv 0$, so that $u_\theta \equiv 0$ and $\sigma_{r\theta} = \sigma_{z\theta} \equiv 0$. The Love function corresponding to some mounting configurations are known in the literature, and are hereafter briefly presented, following the overview proposed by Little in [30].

3. Optimal Mounting Configurations With Null Radial Displacement

In order to identify the optimal mounting configurations, it is useful to analyze first the simplest situation where the disc is uniformly squeezed between two plates. From the elasticity theory point of view, this configuration is a classical problem that does not present any specific difficulty. It is however considered here because it evidences a simple use of the Love strain function, which will be used later in less intuitive configurations. In the case of the compressed disc, the Love strain function is the third order homogeneous polynomial solution of (1), which explicitly reads

$$\mathcal{L}_3 = A_3\left(z^2 - \frac{3}{2}r^2\right)z + B_3(r^2+z^2)z. \tag{4}$$

The stress and displacement fields can be explicitly calculated using Eqs. (2) and (3). All the inner stresses have to be uniformly null except the normal stress σ_{zz}. In particular, setting σ_{rr} and $\sigma_{\theta\theta}$ to zero yields the relationship $3A_3 = -(10\nu - 2)B_3$, which in turn yields $\sigma_{zz} = 10(1+\nu)B_3$. This normal stress also depends on the force F exerted on the top/bottom surface S of the disc, following $\sigma_{zz} = -F/S$. Hence, the coefficient B_3 is straightforwardly obtained as $B_3 = -F/10S(1+\nu)$. The non-null displacement are therefore $u_r = \nu[F/ES]r$ and $u_z = -[F/ES]z$. It is interesting to note that

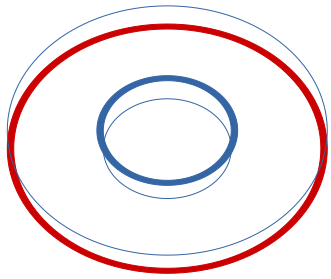

Fig. 2. Schematic representation of the clamped resonator. The red band is supported from below close to the outer radius, while a varying pressure is applied to the top blue band close to the inner radius. In our analysis, we consider a calcium fluoride disc resonator with inner radius $a = 2$ mm, outer radius $b = 5$ mm, and thickness $h = 0.5$ mm. The width of the strips where the disc is clamped is $w = 0.2$ mm.

the radial displacement u_r is not null. In consequence, any fluctuation $\delta F(t)$ of the mounting force would be directly converted into a radius fluctuation $\delta R(t) = [\nu R/ES]\delta F(t)$, which would automatically induce an undesirable frequency fluctuation $\delta f(t) = [f/R]\delta R(t)$, as discussed in the introduction.

As indicated earlier, optimal configurations ideally require the fulfillment of the condition $u_r = 0$ for $z = 0$ and $r = a$. A first option corresponds to the bent disc configuration obeys the following fourth-order polynomial Love strain function

$$\mathcal{L}_4 = A_4\left(z^4 - 3r^2z^2 + \frac{3}{8}r^4\right) + B_4(r^2 + z^2)\left(z^2 - \frac{1}{2}r^2\right). \tag{5}$$

The hypothesis of a bent cylinder with free-load top and bottom boundaries requires $\sigma_{zz} \equiv 0$. This condition yields a uniformly null shear stress $\sigma_{rz} = 0$, so that the non-null components of the stress and displacement fields are $2G\ u_r = 14(1-\nu)B_4\, rz$; $2G\ u_z = \left[-14\nu z^2 + (7\nu - 5)\ r^2\right]B_4$; and $\sigma_{rr} = \sigma_{\theta\theta} = 14(1+\nu)B_4\, z$. In this case, the symmetry plane $z = 0$ is not submitted to any radial displacement or stress.

The sheared disc configuration obeys the Love strain function

$$\mathcal{L}_0 = A_0 r^2 \ln r \tag{6}$$

and yields the following displacement and stress fields $2G\ u_r = 0$; $2G\ u_z = 2(1-\nu)[4\ln r - 3]\,A_0$; $\sigma_{rz} = -4(1-\nu)A_0/r$; and $\sigma_{rr} = \sigma_{\theta\theta} = \sigma_{zz} = 0$. This solution does not hold for a full cylinder, as the it diverges at $r = 0$. However, in the case where a hole is drilled at the center of the disc, this solution is valid and correspond to the situation where the disc is in equilibrium through counterbalancing shear stresses on the inner and outer radii a and b.

The preceding two configurations (bent and sheared discs) fulfill the zero-displacement condition needed at the edge of the resonator. They also share another similarity, which is zero normal stress ($\sigma_{zz} = 0$). However, they are unfortunately not easy to realize experimentally, as both solutions require to exert a stress at the external rim of the disc. Since the Q-factor of the resonator critically depends on the rim surface quality, any mounting solution requiring a contact with the rim is definitely not satisfying and has to be discarded.

An intermediate solution, here referred to as the *clamped resonator*, is presented on Fig. 2. On the one hand, this mounting configuration shares similarities with the bent resonator configuration, as it induces a bending torque as well. On the other hand, it also shares similarities with the sheared resonator because the mounting is somewhat equivalent to counterbalancing shear stresses that are very localized near the inner and outer edges of the disc (but not tangentially to the rim, though). Hence, it can be foreshadowed that clamping the disc between two cylinders with different radii could in optimal conditions induce a radial displacement field that is null at the rim of the disc, regardless of the mounting force intensity.

This possibility can in fact be inferred from the Euler-Bernoulli beam theory, which tells that when a beam is loaded (for example bent downwards), the top-half is stretched while the bottom-half is

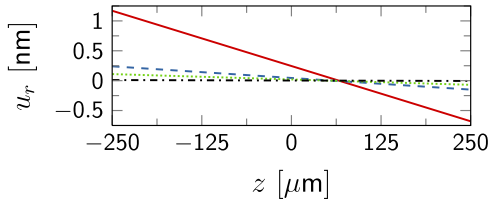

Fig. 3. Plot of $u_r(z)$ along the disc edge for four different values of mounting pressure: 50 Pa (dashed dotted black), 500 Pa (dotted green), 1000 Pa (dashed blue), and 5000 Pa (continuous red). The fact that $u_r(z) = 0$ for $z = 68.4\,\mu$m in all cases suggests that the frequency of a WGM propagating in this region would be independent of mounting pressure.

symmetrically compressed. Therefore, the plane of symmetry does not undergo any longitudinal deformation at the first order. The same phenomenology would occur when a resonator is bent. Theoretical analysis indicates that along the radial displacement field at the edge, the stress and strain fields are also null in this neutral plane. Hence, from an elastostatic point of view, the WGMs are indeed under the physical condition of a load-free resonator regardless of the mounting force.

4. Numerical Simulations

The heuristic analysis presented above provides intuition that a neutral clamping configuration exists for WGM disc resonators. However, to verify this intuition and furthermore provide the quantitative results that would be necessary for designing a physical system for experiment, numerical simulations are necessary.

We performed finite element method (FEM) simulations using COMSOL. Because our co-axially clamped resonator can be thought of as a hybrid of the sheared and bent disc situations, we worked with a geometry where the disc has a central hole. The dimensions of the disc are, inner radius, $a = 2$ mm, outer radius, $b = 5$ mm, and a thickness of 0.5 mm, with the disc symmetry plane aligned on the z axis ($-250\ \mu\text{m} < z < 250\ \mu\text{m}$). We assigned material properties to the disc based on those of calcium fluoride, with Young's modulus $E = 75.8$ GPa, Poisson ratio $\nu = 0.26$, and density $\rho = 3180$ kg m^{-3}.

We performed FEM simulation with a 200 μm wide strip along the top, inner portion of the disc is held from above, while a 200 μm wide strip along the outer, lower portion of the disc is supported from below (see Fig. 2). The boundary condition along the lower support calls for zero vertical displacement, but lateral displacement is permitted. This is physically described as a rigid support upon which the disc surface, under deformation, can slide without friction. The mounting surface at the top is a "fixed" boundary condition, and no lateral or vertical displacement is allowed here. This is an approximation of the physical situation where the disc is glued to the top mount.

Deformation of the mounting structure changes the effective force applied to the disc. This is modeled by applying a force in the positive z direction F_z to the bottom mounting surface. The magnitude of this force is then varied, and the resulting deformations of the disc resonator are analyzed (see Fig. 3).

Results of the FEM simulation confirm the existence of a location at the edge of the disc where radial deformation is zero for a wide range of mounting-force values. Simulations indicate that there is effectively a crossing-point in the thickness of the disc where the radial displacement is null. Fig. 3 shows radial deformation $u_r(z)$ plotted along the edge of the disc for mounting-forces spanning two orders of magnitude. In all cases, the disc does not deform radially at a position 64.8 μm above the mid-plane of the disc. As explained in Sections 1 and 2, the existence of this turning point is *per se* a guaranty of immunity to small vibrations. However, this clamped architecture provides even superior immunity, as the turning point remains exactly the same for a very wide range of mounting force amplitudes.

Beside radial displacement, it is noteworthy that both the radial stress and strain are (quasi-)null in the same area. In other words, the clamped disc undergoes zero displacement, stress and strain in the radial direction: in this case, the loaded disc is almost totally immune to the mounting

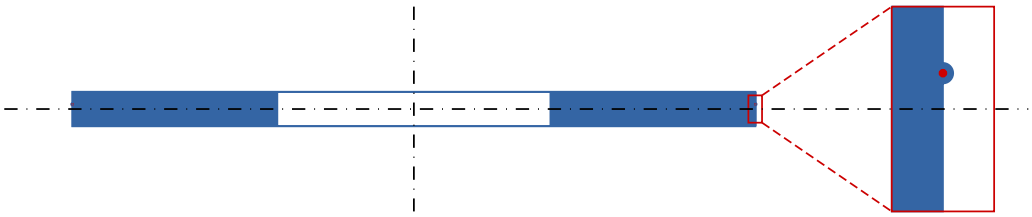

Fig. 4. Schematic side-view of the disc-resonator of Fig. 2 optimized according to the results shown on Fig. 3. A torus-like protuberance (with a local curvature radius of 20 μm) is created at the robust turning of height $z = 68.4\ \mu$m (see the enlargement). The eigenfrequency of a WGM located within that protuberance (red dot) would be insensitive to vibrations transmitted by the mounting force.

forces in the area of interest (torus-like tube were are located the WGMs), as it behaves as the load-free disc. These simulations results are in qualitative agreement with the theoretical analysis led for the bent and sheared discs. The fact that the turning point remains the same even when the loading force spans across two orders of magnitude is a reliable indicator of the robustness of this mounting scheme, which is therefore valid far beyond the approximation of first order perturbations. In particular, it proves that the system would be very insensitive to low-frequency vibrations (which induce only small load variations), but also to large accelerations (which may induce significantly large load variations).

The existence of such a robust turning point also indicates that if the WGMs are traveling at the height of the corresponding turning point, they would not undergo any eigenfrequency shift. Hence, manufacturing a resonator with a single-mode protuberance at that height to host the relevant eigenmodes (see, for example, [32] and [33]) would lead to a force-insensitive cavity, and therefore to a higher frequency stability, as explained in Fig. 4. It is also noteworthy that the location of this turning point does not coincide with the geometric symmetry plane. This is a result of the asymmetric boundary conditions, i.e., that the inner mounting surface is fixed (and the material cannot deform radially), but the outer mounting surface is allowed to deform radially. However, the results are consistent with the intuition from the Euler-Bernoulli theory, which predicts a neutral plane between regions of compression and expansion, where the desired nonlinear and quantum phenomena (see, for example, [34]–[40]) can take place without unwanted external perturbations.

5. Conclusion

In this work, we have investigated a neutral mounting architecture for WGM disc resonators. Theoretical analysis and numerical simulations have shown that optimal configurations exist for maintaining frequency stability for a very wide range of loading force and acceleration. Further theoretical work is needed for the case of anisotropic crystals and/or time-varying loads (see, for example, [41]). The present theoretical analysis, which will have to be confirmed experimentally, indicates that the reduction of vibration- and acceleration-induced frequency fluctuations in WGM disc-resonators can be achieved with a simple mounting scheme. Successful implementation of such device would offer a small and robust frequency reference for portable and practical devices in a non-laboratory environment.

References

[1] I. S. Grudinin *et al.*, "Ultra high Q crystalline microcavities," *Opt. Commun.*, vol. 265, 33–38, 2006.
[2] I. S. Grudinin, V. S. Ilchenko, and L. Maleki, "Ultrahigh optical Q factors of crystalline resonators in the linear regime," *Phys. Rev. A*, vol. 74, 2006, Art. no. 063806.
[3] A. Coillet *et al.*, "Microwave photonics systems based on whispering-gallery-mode resonators," *J. Vis. Exp.*, vol. 78, 2013, Art. no. e50423.
[4] G. Lin, S. Diallo, R. Henriet, M. Jacquot, and Y. K. Chembo, "Barium fluoride whispering-gallery-mode disc-resonator with one billion quality-factor," *Opt. Lett.*, vol. 39, pp. 6009–6012, 2014.

[5] R. Henriet *et al.*, "Kerr optical frequency comb generation in strontium fluoride whispering-gallery mode resonators with billion quality factor," *Opt. Lett.*, vol. 40, pp. 1567–1570, 2015.
[6] T. J. Kippenberg, R. Holzwarth, and S. A. Diddams, "Microresonator-based optical frequency combs," *Science*, vol. 322, pp. 555–559, 2011.
[7] Y. K. Chembo, "Kerr optical frequency combs: theory, applications and perspectives," *Nanophoton.*, vol. 5, pp. 214–230, 2016.
[8] L. Maleki, "The optoelectronic oscillator," *Nature Photon.*, vol. 5, pp. 728–730, 2011.
[9] J. J. Li, H. Lee, T. Chen, and K. J. Vahala, "Low-pump-power, low-phase-noise, and microwave to millimeter-wave repetition rate operation in microcombs," *Phys. Rev. Lett.*, vol. 109, 2012, Art. no. 233901.
[10] P. Del'Haye, S. B. Papp, and S. A. Diddams, "Hybrid electro-optically modulated microcombs," *Phys. Rev. Lett.*, vol. 109, 2012, Art. no. 263901.
[11] A. A. Savchenkov *et al.*, "Stabilization of a Kerr frequency comb oscillator," *Opt. Lett.*, vol. 38, pp. 2636–2639, 2013.
[12] P. Del'Haye, K. Beha, S. B. Papp, and S. A. Diddams, "Self-injection locking and phase-locked states in microresonator-based optical frequency combs," *Phys. Rev. Lett.*, vol. 112, 2014, Art. no. 043905.
[13] W. Liang *et al.*, "High spectral purity Kerr frequency comb radio frequency photonic oscillator," *Nature Commun.*, vol. 6, 2015, Art. no. 7957.
[14] A. B. Matsko and L. Maleki, "Noise conversion in Kerr comb RF photonic oscillators," *J. Opt. Soc. Amer. B*, vol. 32, pp. 232–240, 2015.
[15] A. B. Matsko, A. A. Savchenkov, N. Yu, and L. Maleki, "Whispering-gallery-mode resonators as frequency references. I. Fundamental limitations," *J. Opt. Soc. Amer. B*, vol. 24, pp. 1324–1335, 2007.
[16] A. A. Savchenkov, A. B. Matsko, V. S. Ilchenko, N. Yu, and L. Maleki, "Whispering-gallery-mode resonators as frequency references. II. Stabilization," *J. Opt. Soc. Amer. B*, vol. 24, pp. 2988–2997, 2007.
[17] A. D. Ludlow *et al.*, "Compact, thermal-noise-limited optical cavity for diode laser stabilization at 1×10^{-15}," *Opt. Lett.*, vol. 32, pp. 641–643, 2007.
[18] S. A. Webster, M. Oxborrow, S. Pugla, J. Millo, and P. Gill, "Thermal-noise-limited optical cavity," *Phys. Rev. A*, vol. 77, 2008, Art. no. 033847.
[19] D. V. Strekalov, R. J. Thompson, L. M. Baumgartel, I. S. Grudinin, and N. Yu, "Temperature measurement and stabilization in a birefringent whispering gallery mode resonator," *Opt. Exp.*, vol. 19, pp. 14449–14501, 2011.
[20] J. Alnis *et al.*, "Thermal-noise-limited crystalline whispering-gallery-mode resonator for laser stabilization," *Phys. Rev. A*, vol. 84, 2011, Art. no. 011804.
[21] D. R. Leibrandt *et al.*, "Spherical reference cavities for frequency stabilization of lasers in non-laboratory environments," *Opt. Exp.*, vol. 19, pp. 3471–3482, 2011.
[22] S. Webster and P. Gill, "Force-insensitive optical cavity," *Opt. Lett.*, vol. 36, pp. 3572–3574, 2011.
[23] C. Y. Wang *et al.*, "Mid-infrared optical frequency combs at 2.5 μm based on crystalline microresonators," *Nature Commun.*, vol. 4, 2013, Art. no. 1345.
[24] K Saleh *et al.*, "Phase noise performance comparison between optoelectronic oscillators based on optical delay lines and whispering gallery mode resonators," *Opt. Exp.*, vol. 22, pp. 32158–32173, 2014.
[25] J. Pfeifle *et al.*, "Optimally coherent Kerr combs generated with crystalline whispering gallery mode resonators for ultrahigh capacity fiber communications," *Phys. Rev. Lett.*, vol. 114, 2015, Art. no. 093902.
[26] G. Lin and Y. K. Chembo, "On the dispersion management of fluorite whispering-gallery mode resonators for Kerr optical frequency comb generation in the telecom and mid-infrared range," *Opt. Exp.*, vol. 23, pp. 1594–1604, 2015.
[27] K. Saleh, G. Lin, and Y. K. Chembo, "Effect of laser coupling and active stabilization on the phase noise performance of optoelectronic microwave oscillators based on whispering-gallery-mode resonators," *IEEE Photon. J.*, vol. 7, pp. 1–11, 2015.
[28] A. Chiasera *et al.*, "Spherical whispering-gallery-mode microresonators," *Laser Photon. Rev.*, vol. 4, pp. 457–482, 2010.
[29] H. Vaughan, "The finite compression of elastic solid cylinders in the presence of gravity," *Proc. Roy. Soc. London A*, vol. 321, pp. 381–396, 1971.
[30] R. W. Little, *Elasticity*. Englewood Cliffs, NJ, USA: Prentice-Hall, 1973.
[31] S. B. Papp and S. A. Diddams, "Spectral and temporal characterization of a fused-quartz-microresonator optical frequency comb," *Phys. Rev. A*, vol. 84, 2011, Art. no. 053833.
[32] I. S. Grudinin and N. Yu, "Dispersion engineering of crystalline resonators via microstructuring," *Optica*, vol. 2, pp. 221–224, 2015.
[33] J. M. Winkler, I. S. Grudinin, and N. Yu, "On the properties of single-mode optical resonators," *Opt. Exp.*, vol. 24, pp. 13231–13243, 2016.
[34] Y. K. Chembo, D. V. Strekalov, and N. Yu, "Spectrum and dynamics of optical frequency combs generated with monolithic whispering gallery mode resonators," *Phys. Rev. Lett.*, vol. 104, 2010, Art. no. 103902.
[35] A. Coillet *et al.*, "Azimuthal turing patterns, bright and dark cavity solitons in Kerr combs generated with whispering-gallery mode resonators," *IEEE Photonics J.*, vol. 5, 2013, Art. no. 6100409.
[36] T. Herr *et al.*, "Temporal solitons in optical microresonators," *Nature Photon.*, vol. 8, pp. 145–152, 2014.
[37] G. Lin *et al.*, "Cascaded Brillouin lasing in monolithic barium fluoride whispering gallery mode resonators," *Appl. Phys. Lett.*, vol. 105, 2014, Art. no. 231103.
[38] Y. K. Chembo, I. S. Grudinin, and N. Yu, "Spatiotemporal dynamics of Kerr–Raman optical frequency combs," *Phys. Rev. A*, vol. 92, 2015, Art. no. 043818.
[39] W. Liang *et al.*, "Miniature multioctave light source based on a monolithic microcavity," *Optica*, vol. 2, pp. 40–47, 2015.
[40] Y. K. Chembo, "Quantum dynamics of Kerr optical frequency combs below and above threshold: Spontaneous four-wave mixing, entanglement, and squeezed states of light," *Phys. Rev. A*, vol. 93, 2016, Art. no. 033820.
[41] M. Eskandari-Ghadi and R. Y. S. Pak, "Axisymmetric body-force fields in elastodynamics of transversely isotropic media," *J. Appl. Mech.*, vol. 76, 2009, Art. no. 061016.